



HAL
open science

Obesogen effect of bisphenol S alters mRNA expression and DNA methylation profiling in male mouse liver

Axelle Brulport, Daniel Vaiman, Marie-Christine Chagnon, Ludovic Le Corre

► To cite this version:

Axelle Brulport, Daniel Vaiman, Marie-Christine Chagnon, Ludovic Le Corre. Obesogen effect of bisphenol S alters mRNA expression and DNA methylation profiling in male mouse liver. *Chemosphere*, 2020, 241, pp.125092. 10.1016/j.chemosphere.2019.125092 . hal-02325508

HAL Id: hal-02325508

<https://institut-agro-dijon.hal.science/hal-02325508>

Submitted on 21 Dec 2021

HAL is a multi-disciplinary open access archive for the deposit and dissemination of scientific research documents, whether they are published or not. The documents may come from teaching and research institutions in France or abroad, or from public or private research centers.

L'archive ouverte pluridisciplinaire **HAL**, est destinée au dépôt et à la diffusion de documents scientifiques de niveau recherche, publiés ou non, émanant des établissements d'enseignement et de recherche français ou étrangers, des laboratoires publics ou privés.



Distributed under a Creative Commons Attribution - NonCommercial 4.0 International License

21 **Abstract**

22 Environmental pollution is increasingly considered an important factor involved in the
23 obesity incidence. Endocrine disruptors (EDs) are important actors in the concept of DOHaD
24 (Developmental Origins of Health and Disease), where epigenetic mechanisms play crucial
25 roles. Bisphenol A (BPA), a monomer used in the manufacture of plastics and resins is one of
26 the most studied obesogenic endocrine disruptor. Bisphenol S (BPS), a BPA substitute, has
27 the same obesogenic properties, acting at low doses with a sex-specific effect following
28 perinatal exposure. Since the liver is a major organ in regulating body lipid homeostasis, we
29 investigated gene expression and DNA methylation under low-dose BPS exposure. The BPS
30 obesogenic effect was associated with an increase of hepatic triglyceride content. These
31 physiological disturbances were accompanied by genome-wide changes in gene expression
32 (1,366 genes significantly modified more than 1.5-fold). Gene ontology analysis revealed
33 alteration of gene cascades involved in protein translation and complement regulation. It was
34 associated with hepatic DNA hypomethylation in autosomes and hypermethylation in sex
35 chromosomes. Although no systematic correlation has been found between gene repression
36 and hypermethylation, several genes related to liver metabolism were either hypermethylated
37 (*Acs14*, *Gpr40*, *Cel*, *Ppar δ* , *Abca6*, *Ces3a*, *Sgms2*) or hypomethylated (*Soga1*, *Gpihbp1*,
38 *Nr1d2*, *Mlxipl*, *Rps6kb2*, *Esrrb*, *Thra*, *Cidec*). In specific cases (*Hapln4*, *ApoA4*, *Cidec*, genes
39 involved in lipid metabolism and liver fibrosis) mRNA upregulation was associated with
40 hypomethylation. In conclusion, we show for the first time wide disruptive physiological
41 effects of low-dose of BPS, which raises the question of its harmlessness as an industrial
42 substitute for BPA.

43 **Keywords:** bisphenol S, obesogen, perinatal chronic exposure, liver, DNA methylation,
44 transcriptome.

45

46 **1. Introduction**

47 Obesity is steadily increasing in many countries around the world. The positive
48 correlation between obesity incidence and the increase in environmental pollution [1] initiated
49 the concept of obesogens [2]. By promoting adipogenesis, these molecules potentiate a pre-
50 existing imbalance in the energy homeostasis [3, 4]. Most obesogens are known to be
51 endocrine disruptors (EDs). As EDs, they can act at low doses (corresponding to
52 environmental doses) and following perinatal exposures [5]. EDs are a common factor in the
53 DOHaD concept (Developmental Origins of Health and Disease) through potential effects of
54 the gestational microenvironment during embryonic and/or fetal development on the
55 occurrence of pathology during adulthood [6].

56 Bisphenol S (BPS), a structural analogue of Bisphenol A (BPA), is commonly used as
57 a substitute for BPA in food contact material (including baby bottles), papers products, paints
58 and varnishes, resins and glues, medical equipment and electronic and electrical components.
59 BPS is ubiquitous in the environment as it was found in indoor air, surface water, sediment,
60 sewage sludge and food). Dietary intake is the main source of BPS human exposure [7]. BPS
61 exhibits a higher body burden, bioavailability and stability in environment than BPA [8]. BPA
62 has obesogenic properties with disparities according to the exposure window, the doses, route
63 of exposure and sex of the animals [3, 9]. Several studies suggested that obesogens induce an
64 overweight only after perinatal exposure in rodent models [4]. BPS induces a similar
65 obesogen effect to BPA following perinatal and chronic exposure at low doses (1.5 µg/kg
66 bw/d) [10].

67 The BPS detection in U.S. adult urine samples increased from 25% to 74% between
68 2000 and 2014 [11]. Using data from BPS urine sample rates and pharmacokinetic models,

69 human BPS exposure could correspond to daily intakes (median values) of 0.023 $\mu\text{g}/\text{d}$ for
70 Korean, 0.316 $\mu\text{g}/\text{d}$ for Americans and 1.67 $\mu\text{g}/\text{d}$ for Japanese [12].

71 It is admitted that when a pregnant female is exposed to a chemical substance, this
72 substance, if small enough, will be able to reach the fetuses via the blood flow and through the
73 placenta. It is also supposed that when an endocrine disrupter mimics the structure of an
74 hormone, it will hijack all its signaling cascade in a atopic and achronic fashion which may
75 explain the pathogenic effect of the exposure.

76 Epigenetic mechanisms like DNA methylation have been associated in the
77 development of obesity in the context of DOHaD [12]. DNA methylation of CpG islands is an
78 important epigenetic mechanism associated with stable long-term changes in gene expression
79 [13]. Several EDs are reported to induce epigenetic changes, notably after perinatal exposure.
80 Thus, it has been described that BPA causes hypomethylation of liver DNA and alters the
81 methylation level of certain CpG sites (notably around transcription start site) of genes
82 involved in liver metabolism [13, 14, 15, 16, 17]. It has been shown for genes involved in
83 glycolysis (hypermethylation of Glucokinase (Gck)), β -oxidation (hypo and hypermethylation
84 of Carnitine Palmitoyltransferase (Cpt1a)) and lipid synthesis (hypomethylation of Nuclear
85 factor E2-related factor (Nrf2) and sterol regulatory element binding protein (Srebf1 and 2))
86 [13, 15, 16, 17]. Recent articles suggest that genome-wide methylation analysis can identify
87 epigenetic biomarkers (gene, transposon) that are indicative of a type of perinatal exposure
88 and predict its consequences in adulthood [18, 19].

89 While the epigenetic effects of BPA are now well evaluated, those of BPS are missing.
90 Here, we analyzed the liver transcriptome and DNA methylation induced by BPS exposure in
91 obesogen conditions. Thus, we performed a perinatal and chronic exposure at BPS low-dose
92 (1.5 $\mu\text{g}/\text{kg}$ body weight/d) in male mice fed with a high fat diet.

93

94 **2. Materials and methods**

95 *2.1. Animals and materials*

96 Pregnant C57Bl/6J mice were purchased from Charles Rivers (L'Arbresle, France). Bisphenol
97 S (BPS) was provided by Sigma-Aldrich (Saint Quentin Fallavier, France). The high fat diet
98 (HFD) was based on the 4RF25 reproduction diet (Mucedola, Milano, Italia) with the addition
99 of palm oil (La Vie Saine, Dijon, France) and cholesterol from Sigma Aldrich (Saint Quentin
100 Fallavier, France).

101

102 *2.2. Experimental design*

103 BPS exposure was performed as previously described [10]. Briefly, eleven pregnant C57Bl/6J
104 mice were divided into two groups and exposed to BPS or not in their drinking water from the
105 first day of gestation (GD0, determined by vaginal plug detection). BPS was dissolved in
106 absolute ethanol (0.1%). Control group drinking water contained only 0.1% ethanol. The
107 treatment was continued during the lactation and in pups after weaning until they were 22-
108 weeks old. At the weaning, the male offspring were divided into two groups. Seventeen and
109 fifteen male mice were included in BPS exposed group and in the control group, respectively.
110 At 8-weeks old, all pups were fed with a high fat diet (60% Kcal from lipids; composed by
111 4RF25 reproduction diet added with 30% palm oil and 0.42g/kg of cholesterol). A maximum
112 of five mice were housed in each cage. The litters were mixed randomly after weaning in
113 order to minimize a possible litter effect. In a cage, each mouse came from a different dam.
114 Under our conventional animal facility conditions, BPS is stable for more than seven days in
115 drinking water. So, we used a concentration of 12.76 ng/ml to obtain an average BPS intake
116 of 0.99 (± 0.057) $\mu\text{g}/\text{kg}$ bw/d for an expected dose of 1.5 $\mu\text{g}/\text{kg}$ bw/d. Cages and bottles were
117 made of polypropylene (bisphenol-free). All mice (fasted 4h before) were sacrificed at 22-
118 weeks old. Before sacrifice, the body weight was measured. At the sacrifice, the livers were

119 weighed, then immediately frozen in liquid nitrogen and stored at -80 °C. Experimental
120 protocol was approved by the ministry and the University of Burgundy's ethic committee.
121 Animal experiments have been carried out in accordance with EU Directive 2010/63/EU for
122 animal experiments.

123

124 *2.3. Liver triacylglycerol assay*

125 Triacylglycerols (TG) were extracted from mouse liver (75 up to 190 mg) according to
126 Schwartz D.M and Wolins N.E [20, 21] and as previously described [22]. Infinity TG®
127 reagent (200 µl, Thermo Fischer Scientific, Asnières sur Seine, France) was used to reveal TG
128 and absorbance at 500 nm was measured using a microplate reader (MultiskanGo®, Thermo-
129 Scientific, France). A calibration curve was generated using a triglyceride standard (FS 200
130 mg/dl, DiaSys, Condom, France). Analysis was carried out in collaboration with the
131 lipidomics platform of Université de Bourgogne Franche-Comté (Dr Jean-Paul Pais de
132 Barros, Dijon, France).

133

134 *2.4 RNA extraction and microarray analysis*

135 Lysis of liver samples from each mouse was performed using Lysing Matrix D™
136 tubes (MP Biomedical, Illkirch-Graffenstaden, France) and the tissue homogenizer
137 Precellys™24 (Bertin technologies, Montigny-le-Bretonneux, France). Total RNA was
138 extracted using Tri-reagent™ (Sigma-Aldrich, Saint Quentin Fallavier, France). RNA
139 quantification and quality were performed by capillary electrophoresis (Agilent bioanalyzer
140 2100, Les Ullis, France). Isolated cRNA of three points per condition was analyzed for global
141 gene expression using Affymetrix Clariom S array hybridization, in the same batch, at the
142 Genomics Platform of the Cochin Institute according to standard validated protocols. Each
143 sample is a liver RNA pool prepared from three distinct mice originating from separate litters.

144 All genes significantly deregulated with a p-value ≤ 0.05 were converted to ENSEMBL ID
145 using Biomart and mm10 version of the mouse genome (<http://www.ensembl.org/biomart>).
146 Liver RNA was extracted from the medial liver lobe whatever the mouse. The platform
147 generated .CEL files that were analyzed using the TAC4.0 (Transcription Analysis Console)
148 from Affymetrix (Applied Biosystems).

149

150 *2.5 Bioinformatics analysis of the expression deregulations*

151 Analysis of the transcriptome for microarray was carried out using two complementary
152 approaches: DAVID analysis of deregulated genes and Functional Gene Set Enrichment using
153 string (<http://string-db.org/>).

154

155 *2.6. DNA extraction*

156 Lysis of liver sample were performed using Lysing Matrix D™ tubes (MP Biomedical,
157 Illkirch-Graffenstaden, France) and the tissue homogenizer Precellys™24 (Bertin
158 technologies, Montigny-le-Bretonneux, France). All sample were treated with 20 µl of
159 proteinase K (20 mg/ml) overnight and with 9 µl of RNase A (20 mg/ml) and 300 U of RNase
160 T1, 30 min at 37 °C just before the DNA extraction using GenElute Mammalian Genomic
161 DNA Miniprep kit™ (Sigma Aldrich, Saint Quentin Fallavier, France) in compliance with the
162 manufacturer's guidelines. Liver DNA was extracted from the medial liver lobe whatever the
163 mouse.

164

165 *2.7. Reduced Representation Bisulfite Sequencing (RRBS)*

166 Reduced Representation Bisulfite Sequencing was performed by Diagenode's DNA
167 Methylation Profiling (RRBS Service) (Diagenode Cat# G02020000). For each group, three
168 samples were analyzed. Each sample is a liver DNA pool prepared from three distinct mice

169 from separate litters. DNA concentration of the samples was measured using the Qubit®
170 dsDNA BR Assay Kit (Thermo Fisher Scientific) and DNA quality was analyzed using the
171 Fragment Analyzer™ and the DNF-487 Standard Sensitivity Genomic DNA Analysis Kit
172 (Advanced Analytical). The library preparation, bisulfite conversion and amplification were
173 performed using Diagenode's Premium RRBS Kit (Diagenode Cat# C02030033) by
174 following manufacturer's recommendations. Finally, RRBS library pools were sequenced on
175 a HiSeq3000 (Illumina) using 50 bp single-read sequencing (SR50).

176 The sequenced reads were controlled for quality of sequencing with FastQC [23]. Adapter
177 removal was performed using Trim Galore! version 0.4.5_dev [24]. The cleaned reads were
178 then aligned to the *Mus musculus* reference genome (Genome Reference Consortium m38
179 (mm10)) using bismark v0.16.1 [25]. Similarly, the sequenced reads were first transformed
180 into the forward and reverse bisulfite converted versions and aligned to the four bisulfite
181 genomes. The reads, producing a unique best hit to one of the bisulfite genomes, were then
182 compared to the unconverted genome. The `cytosine2coverage` and
183 `bismark_methylation_extractor` modules of bismark were used to infer the methylation state
184 of all cytosines in a CpG context (for every single mappable read) and to compute the
185 percentage methylation for each CpG site. The spike-in control sequences were used at this
186 step to check the bisulfite conversion rates and to validate the efficiency of the bisulfite
187 treatment (supplementary data A1).

188 Methylkit [26], a R/Bioconductor package, was used to perform the differential methylation
189 analysis. The CpG data set was filtered for low coverage (CpGs with coverage less than 10X
190 were discarded) and for extremely high coverage to discard reads with possible PCR bias
191 (CpGs with coverage higher than the 99.9th percentile were discarded). Pairwise comparisons
192 were performed to identify differentially methylated CpGs (DMC) and differentially
193 methylated regions (DMRs), the latter with a window and step size of 1000 bp. DMCs and

194 DMRs with a percent methylation difference higher than 25% and a q-value smaller than 0.01
195 were considered statistically significant. DMCs were annotated with the R/Bioconductor
196 package annotatr [27], with the mm10 refGene and CpG island annotations from UCSC [28].
197 The annotation comprised two categories: (i) distance to a CpG island and (ii) regional
198 annotation. The distance related annotation classified DMCs and DMRs whether they
199 overlapped a known CpG island, 2000 bp of the flanking regions of the CpG islands (shores),
200 2000bp of the flanking regions of the shores (shelves) or outside these regions (open sea). The
201 regional analysis classified DMCs in four groups, namely, exons, introns, promoters and
202 intergenic regions.

203

204 *2.8. Statistical analysis*

205 All data were expressed as mean \pm standard error of mean (SEM). To determine the
206 statistically significant difference between two groups, a Student's unpaired *t*-test was used
207 after checking that the data assumed Gaussian distributions and equal variances with Graph
208 Pad Prism® software and RStudio® software. Results were considered statistically significant
209 at $p < 0.05$.

210

211 **3. Results**

212

213 *3.1. BPS obesogenic effect is correlated with an increase of hepatic triglyceride*
214 *content.*

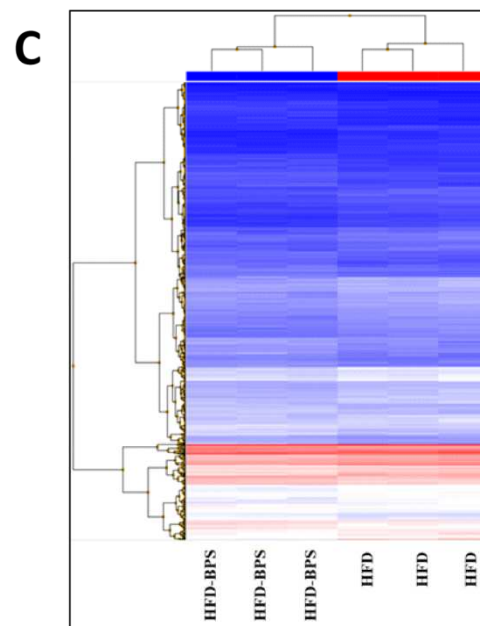
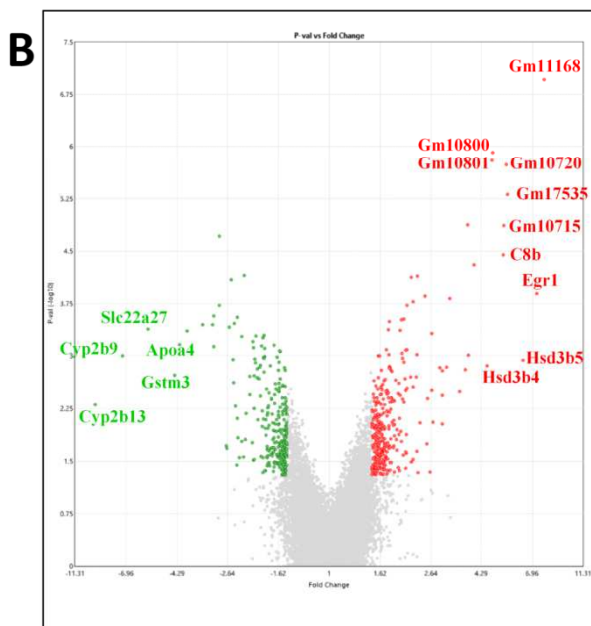
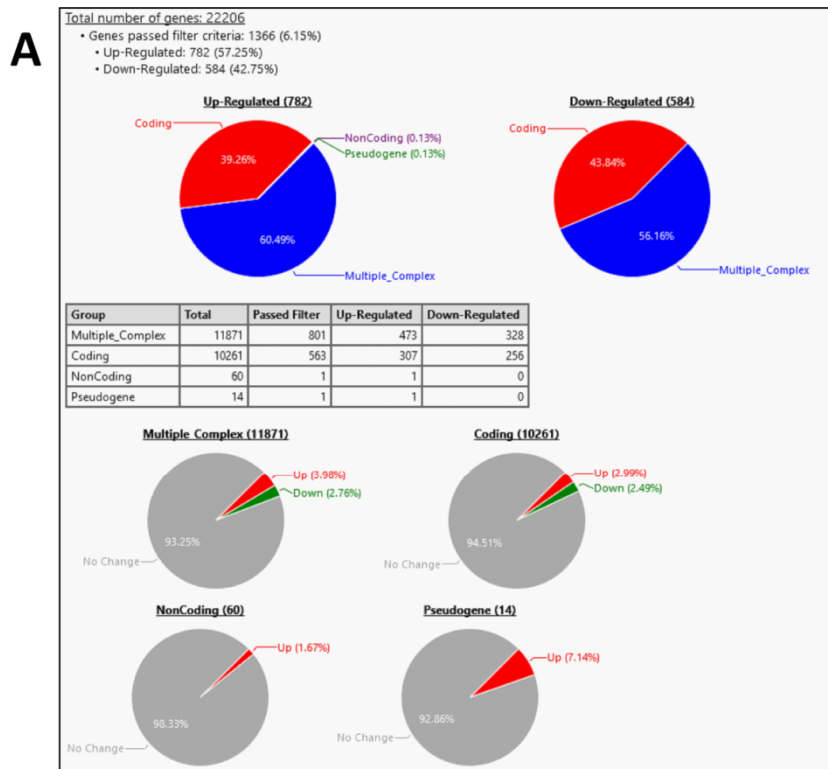
215 In a previous study, we reported a significant increase in body weight (from 38.93 g to
216 46.44 g, a fold increase of 1.2 ± 0.02 ; $p < 0.001$) only in male mice fed a high fat diet and
217 exposed to BPS in comparison with unexposed male mice also fed with a high fat diet. This
218 obesogen effect of BPS was positively correlated with the body fat mass [10]. In male mice

219 fed with a fat diet, the BPS-induced overweight is associated with a hepatic triglyceride
220 content significantly increased (268.23 mg to 731.79 mg, a 2.7 ± 0.5 -fold increase; $p < 0.05$)
221 and a weak increase but not statistically significant on the liver weight (1.2-fold increase;
222 supplementary data A2).

223

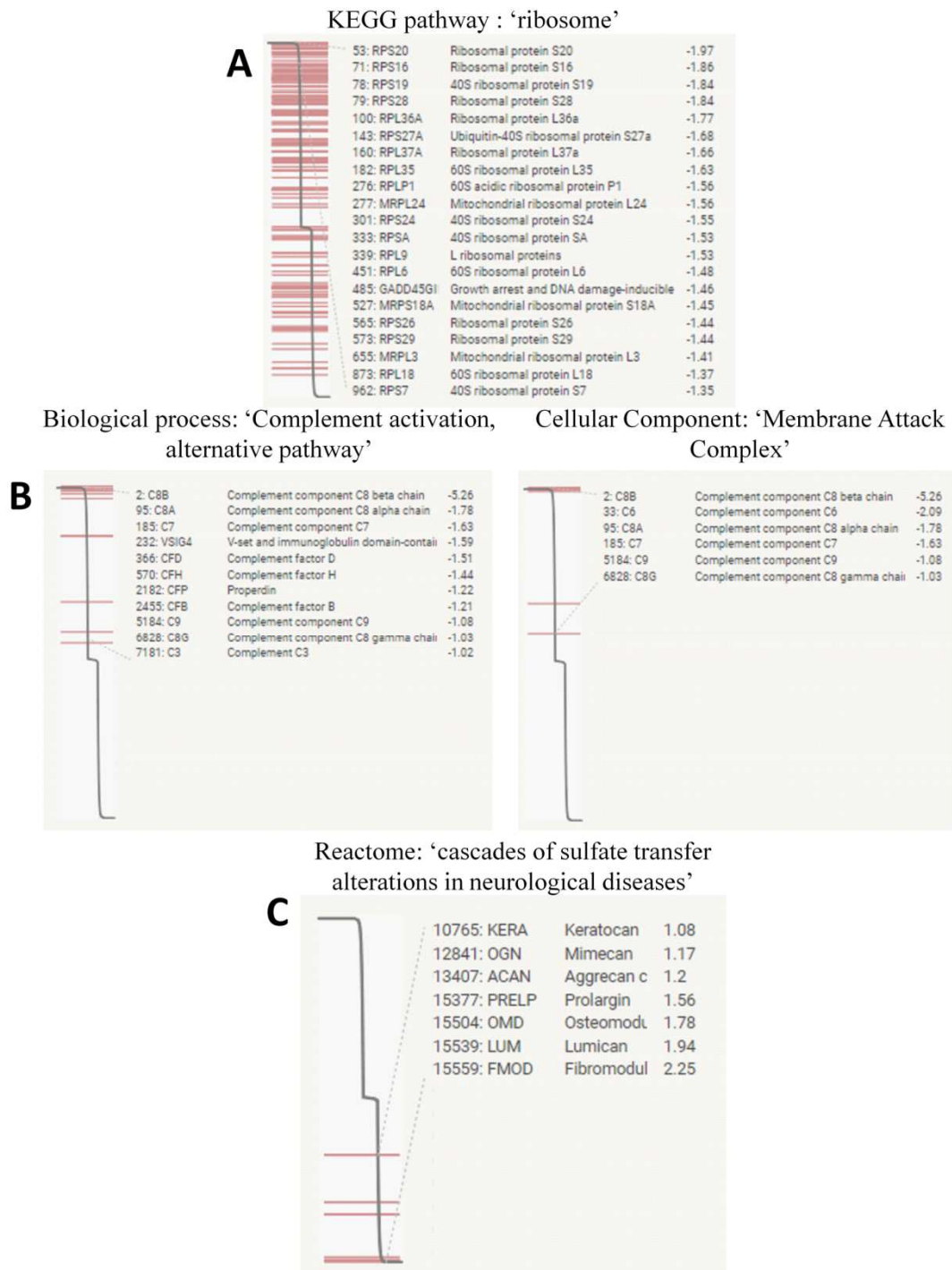
224 *3.2 mRNA differential expression profiling of liver genes*

225 Amongst 22,206 genes using a threshold of 1.5-fold and a p value < 0.05 , 1,366 genes
226 were found deregulated (782 up-regulated and 584 down-regulated, Figure 1A). Among these
227 genes, most belong to the categories Coding and Multiple Complex, logically since they are
228 mainly interrogated by this microarray design. The most up-regulated mRNAs were
229 Cytochrome P450 Family 2 Subfamily B Member 13 (Cyp2b13), Cytochrome P450 Family 2
230 Subfamily B Member 9 (Cyp2b9), Solute Carrier Family 22 Member 27 (Slc22a27),
231 Glutathione S-Transferase Mu 3 (Gstm3) and Apolipoprotein A4 (ApoA4) (up-regulated by
232 BPS in the HFD condition more than 4 fold), while the more strongly decreased mRNAs were
233 Hydroxy-Delta-5-Steroid Dehydrogenase, 3 Beta- And Steroid Delta-Isomerase 4 (Hsd3b4),
234 Gm10800, Gm10801, C8 beta chain (C8b), Gm10715, Gm10720, Gm17535, Hydroxy-Delta-
235 5-Steroid Dehydrogenase, 3 Beta- And Steroid Delta-Isomerase 5 (Hsd3b5), Early growth
236 response 1 (Egr1) and Gm11168 (that are decreased more than 4 fold), as shown in Figure 1B.
237 To note, these Gm genes belong to two clusters located on chromosome 2 for Gm10800 and
238 Gm10801 and on chromosome 9 for Gm10715, Gm10720, Gm17535 and Gm11168,
239 suggesting that their deregulation may be associated with specific cis-elements. Sequence
240 analysis of the proteins encoded by these genes suggest a membrane localization since they
241 harbor four to five putative transmembrane domains. Using a semi-supervised analysis on the
242 1366 differential genes, it was possible to classify unambiguously the effects of BPS
243 superimposed on the high fat diet (Figure 1C).



244 Figure 1. (A) Expression profiling of liver up-regulated or down-regulated genes according to their category and
 245 (B) their level of deregulation in volcano plot (up-regulated more than 4 fold in green (left panel) and down-
 246 regulated more than 4 fold in red (right panel)). (C) Heatmap of differently expressed genes (C) when liver
 247 mRNA of C57Bl/6J male mice fed with a high fat diet and after BPS exposure from GD0 to 22 weeks-old at 1.5
 248 $\mu\text{g}/\text{kg}$ bw/d (HFD BPS 1.5) was compared with liver mRNA of HFD control mice by microarray. $n = 9/\text{group}$.
 249

250 To further understand the alterations of gene functions triggered by BPS treatment we
251 performed a Gene Set Enrichment Analysis using the recently developed tool of the web-
252 based String tool (<https://string-db.org/cgi/input.pl?sessionId=Zdoso9cqhBbX>). We
253 performed two kinds of analyses using either the total gene set (Analysis A: 15,582 genes
254 were recognized by the software), or the gene set limited to the 1,366 significant genes
255 (Analysis B: 1,021 recognized genes). In the A analysis (summarized in Figure 2), a
256 systematic keyword, 'ribosome', came out from various databases (Molecular Function,
257 Cellular Component, Uniprot, KEGG), corresponding to genes that are almost systematically
258 down-regulated involved in ribosomal function, and thus in protein translation and dynamics
259 (Figure 2A). We could also note a systematic enrichment of complement function down-
260 regulated genes, as well as Membrane Attack Complex [focused as well on the C9
261 complement component that corresponds to the generation of a membrane pore before the cell
262 destruction (Figure 2B)]. Complement activation is a very general stress response pathway
263 often activated following various exposures. By contrast, rarer pathways were found enriched
264 in the Reactome database in genes that are overexpressed following BPS exposure especially
265 associated to the transfer of sulfate residues and their implication in diseases (mental
266 retardation, infantile epileptic encephalopathy, macular corneal dystrophy) as shown in Figure
267 2C.

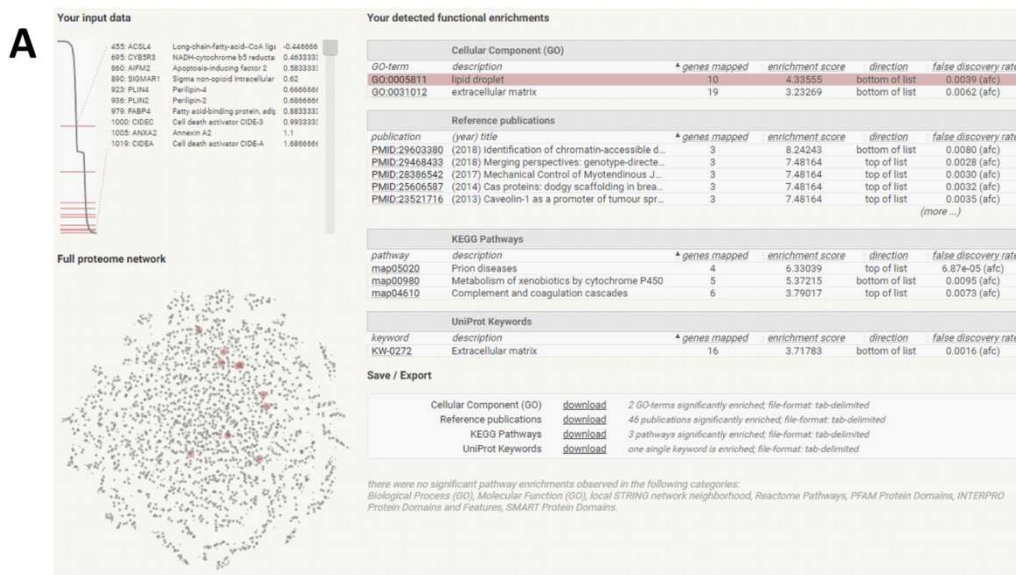


268 Figure 2. Functional Gene Set Enrichment Analysis for down-regulated genes (A, B), and overexpressed genes
 269 (C) using the total gene set when we compare liver mRNA of C57Bl/6J male mice fed with a high fat diet and
 270 after BPS exposure from GD0 to 22 weeks-old at 1.5 $\mu\text{g}/\text{kg}$ bw/d (HFD BPS 1.5) with liver mRNA of HFD
 271 control mice by microarray. n = 9/group.

272

273 When the analysis was only focused on the 1,366 significant genes, lipid droplets
 274 component appeared as the most enriched cellular component in up-regulated genes (Figure

275 3A), which is consistent with the increase of hepatic triglycerides content, revealing specific
 276 alterations of lipid metabolism in the mice exposed to BPS under a high-fat diet. Amongst the
 277 KEGG pathways the alterations of the complement cascade were again found using the
 278 transcriptome data restricted to the significant genes (Figure 3B).



KEGG pathways: 'Complement and Coagulation cascades'



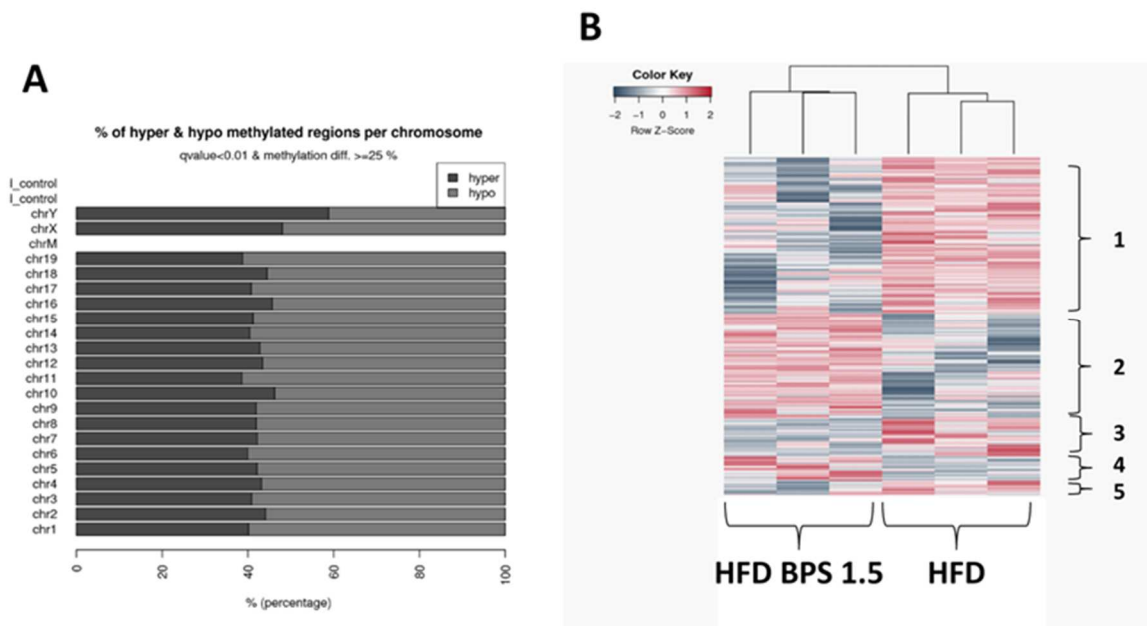
279 Figure 3. Functional Gene Set Enrichment Analysis for up-regulated genes (A), and down-regulated
 280 genes (B) focused on the significant genes when liver mRNA of C57Bl/6J male mice fed with a high fat diet and
 281 after BPS exposure from GD0 to 22 weeks-old at 1.5 µg/kg bw/d (HFD BPS 1.5) was compared with liver
 282 mRNA of HFD control mice by microarray. n = 9/group.

283

284 3.3. *Untargeted assessment of genome-wide alterations in liver DNA methylation by*
285 *Reduced Representation Bisulfite Sequencing (RRBS)*

286 To investigate whether changes in DNA methylation in the liver were induced by BPS
287 and HFD, we analyzed the liver DNA of these mice by RRBS allowing to analyze the genome
288 part ($\approx 1\%$) encompassing 70% of the CpGs islands in mice. Figures 5A and 5B depict the
289 Differentially Methylated Regions (DMRs) that were identified in the data set, with a percent
290 methylation difference cutoff of 25% and q-value of 0.01. The obesogenic effect of BPS in
291 male mice fed with HFD was associated with a significant hypo or hyper methylation of 2,604
292 DMRs (width of 1,000 nucleotides per DMR), which corresponds to 10.42% of the DMRs
293 assessed by the RRBS approach. Among these DMRs observed between the HFD BPS 1.5
294 and the HFD groups, those located in the autosome regions are mainly hypomethylated at
295 61.5% (against 38.5% for hypermethylated regions) (Figure 4A). By contrast,
296 hypermethylation was predominant in the sex chromosomes (Figure 4A).

297 Non-supervised hierarchical classification revealed five clusters of Differentially
298 Methylated Region (DMR) according to the direction of the BPS obesogenic effect (Figure
299 4B). The 1, 3 and 5 clusters contain regions down-methylated by BPS exposure. In contrast,
300 the clusters 2 and 4 contain regions up-methylated by BPS exposure (Figure 4B).



301 Figure 4. Percentage of hyper and hypomethylated regions per chromosome with a percent methylation
 302 difference cutoff of 25% and q-value of 0.01(A), and heatmap of Differentially Methylated Regions (DMRs)
 303 (width of 1000 nucleotides) (B) when liver DNA of C57Bl/6J male mice fed with a high fat diet and after BPS
 304 exposure from GD0 to 22 weeks-old at 1.5 $\mu\text{g}/\text{kg}$ bw/d (HFD BPS 1.5) was compared with liver DNA of HFD
 305 control mice by RRBS. $n = 9/\text{group}$.

306

307 3.4. Genomic distribution of differentially methylated CpGs

308 In the current experiment, between 362 and 522 million of cytosine were analyzed per
 309 sample (data not shown). The methylated/non-methylated cytosine ratios are in the same
 310 range 43% for HFD mice and 42% for BPS exposed mice (data not shown). Among the
 311 cytosines analyzed, 20% is located inside CpGs islands, 22% is in a CpHpG context and 56%
 312 is in a CpHpH context (with H = A, C or T), and this is consistent across all samples and with
 313 standard RRBS results for a mouse sample. Although the cytosines analyzed in the CpG
 314 islands represent only 20% of the cytosines analyzed, more than 40% is methylated, while
 315 only 0.5% to 0.3% of the cytosines in a CpHpG or CpHpH context is methylated, respectively
 316 (data not shown).

317 For the HFD BPS 1.5 vs HFD comparison, 6.8% of differentially methylated CpGs
318 were found located within CpG islands (defined by the following criteria: > 200 bp length,
319 GC percentage > 50% and observed/expected CpG ratio > 60%), 4.3% within CpG shelves
320 (2-4 kb from CpG island), 10.2% within CpG shores (regions up to 2 kb away from CpG
321 islands) and 78.8% in open sea (isolated CpGs in the genome) [29] (Figure 5B). Concerning
322 the gene localization of the alterations, we identified 17.4% of differentially methylated CpGs
323 located in exons, 36.3% in intergenic regions, 41.5% in introns and 4.8% in promoter regions
324 (Figure 5A).

325 Overall, 6,552 fragments were found significantly altered nearby 1,952 genes (some
326 genes being associated with several differentially methylated fragments, Supplementary Table
327 A.1). The genes for which the maximum number of modified fragment was counted, was the
328 complex imprinted gene Gnas (55 fragments), Zinc Finger And SCAN Domain Containing 10
329 (Zscan10: 49 fragments), Apoptosis Associated Tyrosine Kinase (Aatk: 32 fragments), T-Box
330 3 (Tbx3: 32 fragments), Signal-Induced Proliferation-Associated 1 (Sipa1: 30 fragments),
331 Nuclear Factor Of Activated T Cells 2 (Nfatc2: 28 fragments).

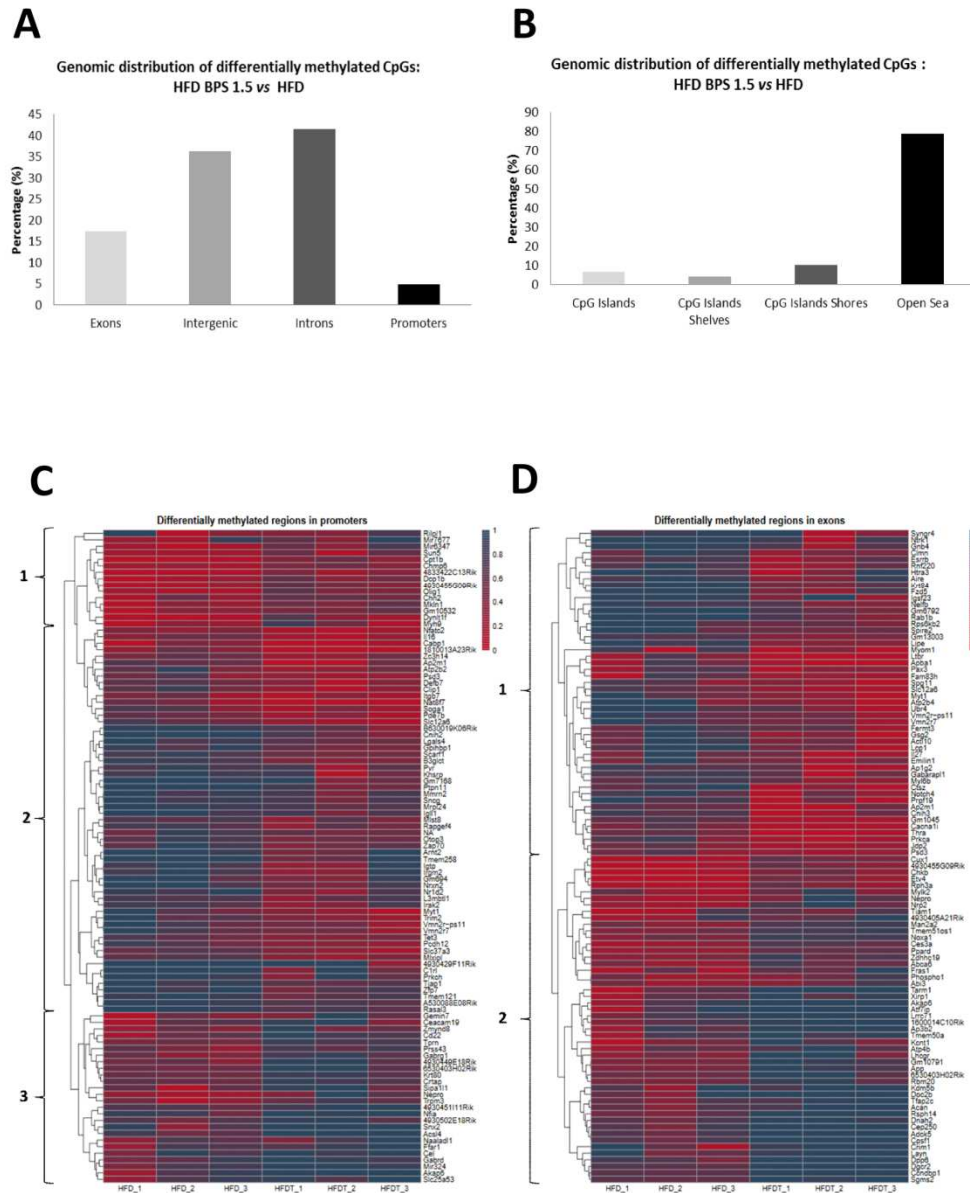
332

333 *3.5. Identification and clustering of genes in differentially methylated regions located*
334 *in promoter areas or exons*

335 The differential methylation in the promoters, allowed us to identify three clusters.
336 Clusters 1 and 3 (Figure 5C) correspond to genes located in hyper-methylated DMRs in the
337 DNA of BPS exposed mice compared to that of unexposed animals. Cluster 2 represents
338 genes located in hypo-methylated DMRs. Several genes involved in liver lipid metabolism are
339 present in this subgroup. Acyl-coA Synthetase Long Chain Family Member 4 (Acsl4)
340 involved in Non-Alcoholic Fatty Liver Disease (NAFLD), free fatty receptor 1
341 (Ffar1/GPR40) implicated in hepatic steatosis and carboxyl ester lipase (Cel) associated to

342 hepatic lipoprotein metabolism present a hyper-methylated promoter. Suppressor of glucose
343 autophagy associated 1 (Soga1) which plays a role in adiponectin-mediated liver insulin
344 sensitivity, glycosylphosphatidylinositol anchored high density lipoprotein binding protein 1
345 (Gpihbp1) controlling hepatic triglyceride content and lipid biosynthetic gene expression,
346 nuclear receptor subfamily 1 group D member 2 (Nr1d2/Rev-Erb-beta) involved in hepatic
347 steatosis related to circadian clock disruption and Mlx interacting protein like (Mlxipl)
348 regulating glycolysis, lipogenesis and gluconeogenesis had hypo-methylated promoters.

349 For exons, only two clusters could be observed (Figure 5D). Ribosomal protein S6
350 kinase beta-2 (Rps6kb2) playing a role in hepatic steatosis and insulin resistance, estrogen
351 related receptor beta (Esrrb) and thyroid hormone receptor alpha (Thra), which are the
352 receptors of two hormones strongly involved in the regulation of energy metabolism, are
353 genes with one or more hypo-methylated exons. Peroxisome proliferator-activated receptor d
354 (Ppard) coordinated regulation of glucose and fatty acid metabolism, ATP-binding cassette a6
355 (Abca6) having an important role in lipid trafficking, carboxylesterase 3a (Ces3a) involved in
356 detoxification and energy homeostasis and sphingomyelin synthase 2 (Sgms2) acting on lipid
357 droplet formation and type 2 diabetes, have one or more exons that are hyper-methylated.



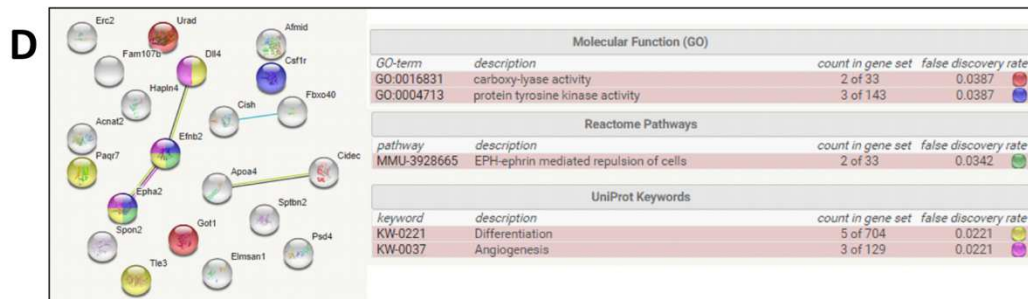
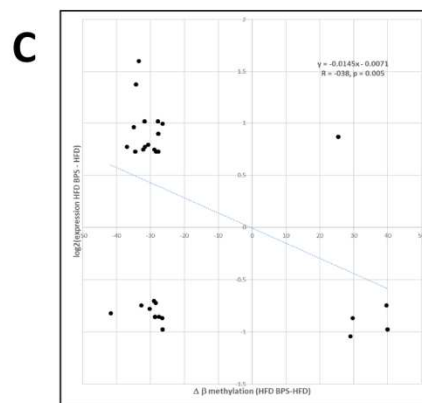
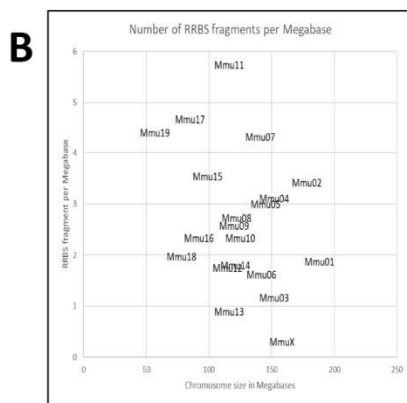
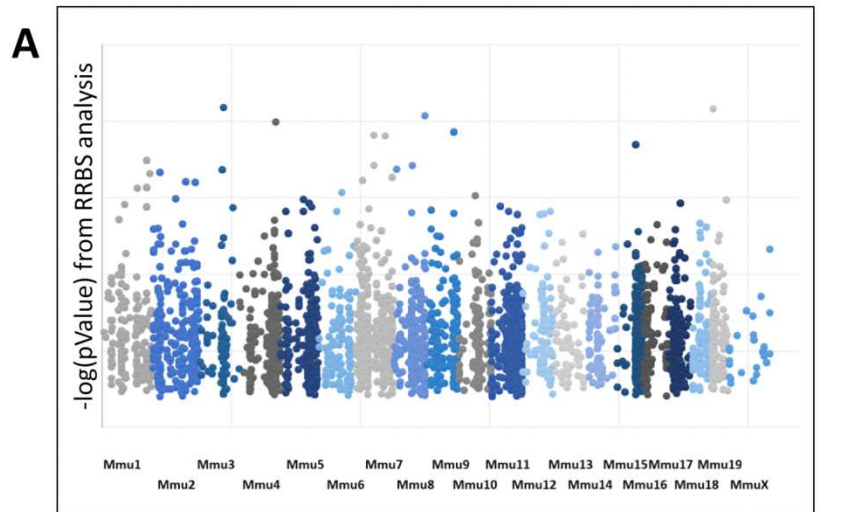
358 Figure 5. The differentially methylated CpGs annotated with different genomic regions (A), as well as CpG
 359 island and shore coordinates (B) and their distribution and heatmaps of top 100 Differentially Methylated
 360 Regions (DMRs) (width of 1000 nucleotides) located in promoters (C) or in exons (D) when liver DNA of
 361 C57Bl/6J male mice fed with a high fat diet and after BPS exposure from GD0 to 22 weeks-old at 1.5 $\mu\text{g}/\text{kg}$
 362 bw/d (HFD BPS 1.5) was compared with liver DNA of HFD control mice by RRBS. (HFD_1 : HFD control
 363 mice sample 1 ; HFDT_1 : HFD exposed to BPS mice sample 1). n = 9/group.

364

365 *3.6. RRBS Hits and connections with gene expression deregulations.*

366 Classically, gene expression is generally thought as down-regulated when CpGs are
 367 methylated. The complete set of differentially methylated RRBS fragments is presented in

368 Figure 6A by following the chromosome distribution (6,552 RRBS fragments). The number
369 of RRBS fragment varied from 44 to 685 (chromosomes X and 11, respectively, Figure 6B).
370 When adjusted to the chromosome size it appears clearly that the density of differential RRBS
371 fragment is not homogeneous according to the chromosome, with the highest density of
372 differential RRBS fragment located on chromosomes 11, 17, 19 and 7. In an attempt to
373 correlate methylation with gene expression, we used a linear regression analysis (Pearson
374 correlation coefficient was calculated and its significance evaluated). When the complete gene
375 expression dataset was matched to the 6552 RRBS fragments, 1958 genes could be identified,
376 but no significant correlation could be found between methylation and gene expression.
377 Selecting genes that are deregulated at the expression level ($\log_2(\text{Delta expression}) > |0.7|$,
378 corresponding ~ 1.62 fold), 71 RRBS fragments were conserved and for them we observed a
379 negative correlation between methylation level and expression for the genes nearby (21 genes,
380 Figure 6C and 6D). These 21 genes were clusterized using String (<https://string-db.org/>), and
381 shown to be involved in important cellular processes, carboxy-lyase and tyrosine kinase
382 activity, cell repulsion mediated by ephrin, differentiation and angiogenesis (Figure 6D).
383 These observations suggest that with HFD, BPS triggers important alterations of the
384 methylation profile with an associated effect on gene expression, but limited to certain genes.



385 Figure 6. Manhattan plot showing the complete set of differentially methylated RRBS fragments following the
 386 chromosome distribution (A), mapping of the density of differential RRBS fragment adjusted to the chromosome
 387 size (B), correlation between DNA methylation and gene expression (C) and Functional Gene Set Enrichment
 388 Analysis for genes with correlation between DNA methylation and expression level when liver mRNA and DNA
 389 of C57Bl/6J male mice fed with a high fat diet and after BPS exposure from GD0 to 22 weeks-old at 1.5 $\mu\text{g}/\text{kg}$
 390 bw/d (HFD BPS 1.5) was compared with liver mRNA and DNA of HFD control mice by microarray and RRBS.
 391 $n = 9/\text{group}$.

392

393

394 4. Discussion

395 In this study, we investigated liver DNA methylation and transcriptomic profiles
396 associated with the obesogen effect of BPS. BPS potentiates the high fat diet-induced obesity
397 in male mice, more specifically after perinatal exposure [30]. Previously, in the male mice fed
398 with HFD and exposed to BPS (1.5 $\mu\text{g}/\text{kg}$ bw/d), we showed that TG and glucose plasma
399 levels were not modified, but insulin and cholesterol plasma levels and HOMA-IR index were
400 significantly increased in comparison with unexposed male mice fed with HFD. So, these
401 mice were in a state of metabolic disturbance characterized by systemic insulin resistance,
402 dyslipidemia, and ectopic storage of fat mass in liver related to the obesogenic effect of BPS
403 [10].

404 Here, we set to a hypothesis-free approaches to evaluate the consequences of the
405 exposition in the liver, through mRNA expression and DNA methylation profiling. Obesity is
406 associated with an increased risk of developing liver disease such as steatosis lesions. The
407 liver plays a key role in lipid metabolism. In the liver, free fatty acids (FFAs) are derived, *via*
408 the portal venous system, from diet, *de novo* lipogenesis from carbohydrates or amino acids
409 and lipolysis in visceral adipose tissue (VAT; [31]. In the hepatocytes, FFAs can be
410 metabolized (β -oxydation) or esterified (storage as triglycerides) or released into the blood
411 flow as very low-density lipoprotein [31]. In addition, the adipokines secreted by VAT and
412 the liver lipid accumulation are susceptible to create an inflammatory state that may promote
413 the development of an insulin resistance context [31]. Furthermore, it's already known that
414 visceral adipose tissue expansion is involved in non-alcoholic fatty liver disease (NAFLD)
415 development [32]. Interestingly, in our study, we observed that the VAT weight was increased
416 in HFD BPS 1.5 mice vs HFD control mice (1.94 g to 2.46 g *i.e* 1.3 \pm 0.05 fold increase) (data
417 not shown). Therefore, these observations suggest that in male mice, the obesity is directly
418 connected with the increase of liver TG. These data are in accordance with previous studies

419 which reported that, *in vitro*, low-concentrations of BPS are able to induce lipid accumulation
420 in murine 3T3L1 preadipocyte cell line [33], but the results are more disputable in hepatic cell
421 lines [34, 35]. However, BPS clearly increases glucose uptake in 3T3L1 preadipocytes and it
422 induces a pro-inflammatory phenotype in the murine macrophage J774A1 lineage [34, 36]. *In*
423 *vivo* and *ex vivo*, BPS affects steroid receptor expression and adipogenesis in adipose tissue
424 and preadipocytes with a sex-specific effect in male sheep [37]. In liver of adult male mice
425 fed with a standard diet, BPS did not affect normalized liver weight at doses ranging between
426 0 and 5000 µg/kg with the highest dose causing histological and pathophysiological damage
427 [38]. Another recent study conducted on female mice adolescent offspring exposed to a low
428 doses of BPS, showed an obesogenic effect of BPS associated with an increase in hepatic
429 triglyceride and cholesterol content without variation of liver weight and with a hepatic
430 glucose homeostasis disturbance [39]. BPS seems to contribute to liver damage associated to
431 obesity by acting on adipose tissue and liver. In addition, a physiologically based
432 pharmacokinetic modeling highlighted that BPS is the BPA substitute which has the most
433 important enterohepatic recirculation leading to poorer urinary excretion [40]. BPS is also the
434 BPA analog leading to the highest internal concentrations of unconjugated bisphenols [40].
435 Its metabolism differs between Humans and mice. In female mice, 50% of the administered
436 BPS is excreted in the urine in 6 h in metabolized form (detoxification mainly in glucuro-
437 conjugated form) [41] In Humans, 92% of BPS is eliminated in non-metabolized form in 48 h
438 in men urine compared to 70% in women urine [42] Consequently, BPS adverse effects can
439 be more critical in Humans than in mice. Hitherto, none of these studies attempted to describe
440 the molecular effect of BPS by high throughput techniques that can provide an unbiased
441 vision of the effects of this molecule.

442 At the molecular level, the transcriptomic analysis that we carried out, shows a
443 decreased mRNA expression of complement components, especially C8b. This gene has

444 recently been identified as a strong novel candidate target for non-alcoholic fatty liver
445 diseases (NAFLD) with a sexual dimorphism [43]. C8b is a target of multiple estrogen
446 receptors ($Esra$, $Esrr\alpha$, $Esrr\beta$, $Esrr\gamma$) which are associated with NAFLD in female mice and
447 affected by testosterone deficiency in male liver [43]. To support this regulatory role of sex
448 hormones, $Hsd3b4$ and $Hsd3b5$, two genes involved in all classes of hormonal steroid
449 biosynthesis are also down-regulated. The second down-regulated key gene $Egr1$ is involved
450 in the metabolism of liver-adipose tissue axis, but data about $Egr1$ function in liver steatosis
451 are contradictory. $Egr1$ deficient mice fed with a high fat diet are less susceptible to diet-
452 induced obesity and obesity-associated disorders (insulin resistance, dyslipidemia and fatty
453 liver) in relation to an increase of energy expenditure in the adipose tissue [44, 45]. In
454 contrast, data from another study showed that increasing $Egr1$ levels in the liver ameliorates
455 diet-induced fatty liver disease in mice, which is more consistent with our observations [46].
456 In addition, $ApoA4$ is strongly up-regulated in our experiment. Interestingly, $ApoA4$
457 participates in liver inflammatory reactions and is an early biomarker of liver fibrosis, which
458 is a critical pathological response to chronic liver disease leading to impairment of liver
459 function [47, 48]. As expected, many of the strongly up-regulated genes $Cyp2b9$, $Cyp2b13$
460 and $Gstm3$ are involved in the detoxification of environmental toxins and in the metabolism
461 of xenobiotics, showing that the liver is actively reacting to the chronic exposure at this BPS
462 low dose [49].

463 Expression alterations in our study occurred through perinatal exposure, suggesting
464 durable epigenome change, in connection with the DOHAD concept [50]. In the present
465 study, we analyzed in parallel the transcriptome and DNA methylation profile after BPS
466 exposure in the liver. All dams were fed with a standard diet, limiting the risk of perinatal
467 effects. Obviously, the risk that the HFD introduced in adulthood interfere with epigenetic
468 changes related to perinatal exposure to BPS exists. Indeed, it has already been shown that the

469 DNA methylation pattern changes with developmental nutritional exposures [51]. Depending
470 on their position, the differently methylated regions will have a variable influence on
471 transcription. Given our knowledge of the mouse genome, we focused our study on the
472 differentially methylated CpGs found on promoters or exons of genes.

473 We showed by RRBS that the obesogenic effect of BPS observed in the male mice
474 was associated with DNA hypomethylation in autosomes and with hypermethylation in sex
475 chromosomes. Overall, 6,552 fragments were found significantly altered, corresponding to
476 1,952 genes (Supplementary Table A3). Alterations in the DNA methylation of these genes
477 constitute a signature of the effect of BPS on the liver, but do not necessarily translate into
478 alterations in gene expression. Concerning the DNA methylations, we identified six genes
479 related to the glucido-lipid metabolism in the liver with one or more hypermethylated CpGs
480 regions in their promoter (*Acs14*, *Gpr40*, *Cel*) or in their exons (*Ppard*, *Abca6*, *Ces3a*, *Sgms2*).
481 Seven other genes involved in the same metabolic functions presented hypomethylated CpGs
482 regions in their promoter (*Soga1*, *Gpihbp1*, *Nr1d2*, *Mlxipl*) or their exons (*Rps6kb2*, *Esrrb*,
483 *Thra*, Cell death activator 3: *Cidec*). Furthermore, two genes involved in liver fibrosis have
484 one or more hypomethylated CpGs regions on their exons (*Hapln4*, *ApoA4*).

485 In the present study, we show that the correlation between DNA methylation and
486 mRNA expression is not always consistent with classical dogma, except when we consider
487 highly deregulated genes. Currently, it is commonly described in the literature (for the liver,
488 see for instance [52]). In the context of gene methylation and expression, several other
489 mechanisms regulating gene expression may be involved, such as post-transcriptional
490 modifications of histones and chromatin rearrangement, as well as aberrant miRNA
491 regulation, remote effect of intron methylations, methylation on repeated sequence impacts
492 and potential role of hydroxymethylation in regulating gene expression [53, 54, 55]]. All of
493 these modifications participate in compression or relaxation processes of chromatin structures

494 that contribute to gene expression regulation [56]. Another potential explanation is linked to
495 the BPS-induced DNA hypomethylation. Indeed, transcribed regions often include functional
496 elements, such as alternative promoters, enhancers, transcription factor binding sites,
497 repetitive elements and enrichment of nucleosomes at intron-exon junctions. Most of these
498 genomic elements are suppressed or stabilized by DNA methylation and hypomethylation
499 may therefore result in their activation and interference with expression of the host gene.
500 However, the demethylation of these elements is only a necessary but not a sufficient
501 condition for them to regain their activities, because the presence of transcription factors
502 specific for these elements (such as highly tissue specific enhancers) is a requirement for their
503 reactivation. Likewise, not all transcription factors are sensitive to DNA methylation
504 occurring within their binding sites [57]. More specifically, in our experimental conditions
505 and from a metabolic point of view, the mice were fasting for 4 h at the time of sacrifice.
506 Hypothetically, this duration allows changes in mRNA expression in the liver (which
507 coordinates metabolic homeostasis by adapting to nutritional status) but not to modify the
508 DNA methylation profile. Indeed, mRNA transcription is a process more dynamic than DNA
509 methylation.

510 Obviously, the effect of BPS on the mRNA expression can be also independent of
511 DNA methylation. Other direct or indirect activity of BPS can occur. Even if the molecular
512 mechanism induced by the BPS are poorly described, many studies reported its endocrine
513 properties. BPS was described to exhibit an estrogenic and anti-androgenic activities by acting
514 directly on sex-hormone receptor [58, 59] or by decreasing basal testosterone secretion by
515 mouse and human fetal testes [60].

516 Most of the molecular mechanisms involved in an integrative approach of epigenetic
517 regulation mechanisms remain to be elucidated. Interestingly, three genes involved in lipid
518 metabolism and liver fibrosis are both upregulated and hypomethylated (Cidec, Hapln4 and

519 ApoA4). Cidec is involved in lipid accumulation in hepatic human and murine cell lines [61,
520 62, 63]. This result is in accordance with the increase of hepatic TG content observed in our
521 study. Hyaluronan and proteoglycan link protein 4 (Hapln4) is involved in formation of
522 extracellular matrix and ApoA4 may be implicated in the evolution of NAFLD in cirrhosis,
523 which is linked to the development of fibrosis [47, 48].

524 To our knowledge, no data are available on the effects of BPS on DNA-specific
525 methylations associated with metabolic disorders. For the first time, in this study, we have
526 demonstrated with an innovative RRBS approach that the obesogenic effect of BPS is
527 associated with global and specific changes in liver DNA methylation, and with the
528 deregulation of expression of genes involved in detoxification, lipid metabolism and protein
529 synthesis. The targets appear to be different from that of BPA although the physiological
530 consequences (obesity, hepatic lipid accumulation, hyperinsulinemia) are quite similar.

531

532

533

534 **Acknowledgments**

535 This work was funded by a grant from the Endocrine Disruptor National Research
536 Program supported by the "Ministère de la transition écologique et solidaire". This work was
537 also funded by Ministère de l'Enseignement Supérieur et de la Recherche (doctoral fellowship
538 to AB) and AgrosupDijon (France). We are grateful to Mr. Guillaume Macquard, Genomic
539 platform of Cochin institute and lipidomic technical platform of Burgundy University for their
540 technical assistance.

541

542 **References**

- 543 1. Baillie-Hamilton PF. Chemical toxins: a hypothesis to explain the global obesity
544 epidemic. *J Altern Complement Med.* 2002 Apr;8(2):185-92. doi:
545 10.1089/107555302317371479. PubMed PMID: 12006126; eng.
- 546 2. Grun F, Blumberg B. Environmental obesogens: organotins and endocrine disruption
547 via nuclear receptor signaling. *Endocrinology.* 2006 Jun;147(6 Suppl):S50-5. doi: en.2005-
548 1129 [pii] 10.1210/en.2005-1129. PubMed PMID: 16690801; eng.
- 549 3. Le Corre L, Besnard P, Chagnon MC. BPA, an energy balance disruptor. *Critical*
550 *reviews in food science and nutrition.* 2015;55(6):769-77. doi:
551 10.1080/10408398.2012.678421. PubMed PMID: 24915348.
- 552 4. Newbold RR, Padilla-Banks E, Jefferson WN. Environmental estrogens and obesity.
553 *Molecular and cellular endocrinology.* 2009 May 25;304(1-2):84-9. doi:
554 10.1016/j.mce.2009.02.024. PubMed PMID: 19433252; PubMed Central PMCID:
555 PMC2682588.
- 556 5. De Coster S, van Larebeke N. Endocrine-disrupting chemicals: associated disorders
557 and mechanisms of action. *Journal of environmental and public health.* 2012;2012:713696.
558 doi: 10.1155/2012/713696. PubMed PMID: 22991565; PubMed Central PMCID:
559 PMC3443608.
- 560 6. Mochizuki K, Hariya N, Honma K, et al. Relationship between epigenetic regulation,
561 dietary habits, and the developmental origins of health and disease theory. *Congenital*
562 *anomalies.* 2017 Nov;57(6):184-190. doi: 10.1111/cga.12213. PubMed PMID: 28169463.
- 563 7. Qiu W, Zhan H, Hu J, et al. The occurrence, potential toxicity, and toxicity mechanism
564 of bisphenol S, a substitute of bisphenol A: A critical review of recent progress.
565 *Ecotoxicology and environmental safety.* 2019 Feb 14;173:192-202. doi:
566 10.1016/j.ecoenv.2019.01.114. PubMed PMID: 30772709.

- 567 8. Danzl E, Sei K, Soda S, et al. Biodegradation of bisphenol A, bisphenol F and
568 bisphenol S in seawater. *International journal of environmental research and public health*.
569 2009 Apr;6(4):1472-84. doi: 10.3390/ijerph6041472. PubMed PMID: 19440529; PubMed
570 Central PMCID: PMC2681201.
- 571 9. van Esterik JC, Dolle ME, Lamoree MH, et al. Programming of metabolic effects in
572 C57BL/6JxFVB mice by exposure to bisphenol A during gestation and lactation. *Toxicology*.
573 2014 Jul 3;321:40-52. doi: 10.1016/j.tox.2014.04.001. PubMed PMID: 24726836.
- 574 10. Ivry Del Moral L, Le Corre L, Poirier H, et al. Obesogen effects after perinatal
575 exposure of 4,4'-sulfonyldiphenol (Bisphenol S) in C57BL/6 mice. *Toxicology*. 2016 May
576 16;357-358:11-20. doi: 10.1016/j.tox.2016.05.023. PubMed PMID: 27241191.
- 577 11. Ye X, Wong LY, Kramer J, et al. Urinary Concentrations of Bisphenol A and Three
578 Other Bisphenols in Convenience Samples of U.S. Adults during 2000-2014. *Environmental
579 science & technology*. 2015 Oct 6;49(19):11834-9. doi: 10.1021/acs.est.5b02135. PubMed
580 PMID: 26360019.
- 581 12. Liao C, Liu F, Alomirah H, et al. Bisphenol S in urine from the United States and
582 seven Asian countries: occurrence and human exposures. *Environmental science &
583 technology*. 2012 Jun 19;46(12):6860-6. doi: 10.1021/es301334j. PubMed PMID: 22620267.
- 584 13. Li G, Chang H, Xia W, et al. F0 maternal BPA exposure induced glucose intolerance
585 of F2 generation through DNA methylation change in Gck. *Toxicology letters*. 2014 Aug
586 4;228(3):192-9. doi: 10.1016/j.toxlet.2014.04.012. PubMed PMID: 24793715.
- 587 14. Kim JH, Sartor MA, Rozek LS, et al. Perinatal bisphenol A exposure promotes dose-
588 dependent alterations of the mouse methylome. *BMC genomics*. 2014 Jan 17;15:30. doi:
589 10.1186/1471-2164-15-30. PubMed PMID: 24433282; PubMed Central PMCID:
590 PMC3902427.

- 591 15. Strakovsky RS, Wang H, Engeseth NJ, et al. Developmental bisphenol A (BPA)
592 exposure leads to sex-specific modification of hepatic gene expression and epigenome at birth
593 that may exacerbate high-fat diet-induced hepatic steatosis. *Toxicology and applied*
594 *pharmacology*. 2015 Apr 15;284(2):101-12. doi: 10.1016/j.taap.2015.02.021. PubMed PMID:
595 25748669; PubMed Central PMCID: PMC4520316.
- 596 16. Shimpi PC, More VR, Paranjpe M, et al. Hepatic Lipid Accumulation and Nrf2
597 Expression following Perinatal and Peripubertal Exposure to Bisphenol A in a Mouse Model
598 of Nonalcoholic Liver Disease. *Environmental health perspectives*. 2017 Aug
599 4;125(8):087005. doi: 10.1289/EHP664. PubMed PMID: 28796629; PubMed Central
600 PMCID: PMC5783659.
- 601 17. Ke ZH, Pan JX, Jin LY, et al. Bisphenol A Exposure May Induce Hepatic Lipid
602 Accumulation via Reprogramming the DNA Methylation Patterns of Genes Involved in Lipid
603 Metabolism. *Scientific reports*. 2016 Aug 9;6:31331. doi: 10.1038/srep31331. PubMed
604 PMID: 27502578; PubMed Central PMCID: PMC4977563.
- 605 18. Anderson OS, Kim JH, Peterson KE, et al. Novel Epigenetic Biomarkers Mediating
606 Bisphenol A Exposure and Metabolic Phenotypes in Female Mice. *Endocrinology*. 2017 Jan
607 1;158(1):31-40. doi: 10.1210/en.2016-1441. PubMed PMID: 27824486; PubMed Central
608 PMCID: PMC5412976.
- 609 19. Faulk C, Kim JH, Anderson OS, et al. Detection of differential DNA methylation in
610 repetitive DNA of mice and humans perinatally exposed to bisphenol A. *Epigenetics*. 2016 Jul
611 2;11(7):489-500. doi: 10.1080/15592294.2016.1183856. PubMed PMID: 27267941; PubMed
612 Central PMCID: PMC4939917.
- 613 20. Danno H, Jincho Y, Budiyanto S, et al. A simple enzymatic quantitative analysis of
614 triglycerides in tissues. *Journal of nutritional science and vitaminology*. 1992 Oct;38(5):517-
615 21. PubMed PMID: 1294711.

- 616 21. Schwartz DM, Wolins NE. A simple and rapid method to assay triacylglycerol in cells
617 and tissues. *Journal of lipid research*. 2007 Nov;48(11):2514-20. doi: 10.1194/jlr.D700017-
618 JLR200. PubMed PMID: 17717377.
- 619 22. Brulport A, Le Corre L, Chagnon MC. Chronic exposure of 2,3,7,8-
620 tetrachlorodibenzo-p-dioxin (TCDD) induces an obesogenic effect in C57BL/6J mice fed a
621 high fat diet. *Toxicology*. 2017 Sep 1;390:43-52. doi: 10.1016/j.tox.2017.07.017. PubMed
622 PMID: 28774668.
- 623 23. Andrews SR. Fast QC: a quality control tool for high throughput sequence data.
624 Available on line at: <http://www.bioinformatics.babraham.ac.uk/projects/fastqc>. 2010.
- 625 24. Krueger F. Trim Galore!: A wrapper tool around Cutadapt and FastQC to consistently
626 apply quality and adapter trimming to FastQ files, with some extra functionality for MspI-
627 digested RRBS-type (Reduced Representation Bisulfite-Seq) libraries. Available on line at:
628 https://www.bioinformatics.babraham.ac.uk/projects/trim_galore/. 2012.
- 629 25. Krueger F, Andrews SR. Bismark: a flexible aligner and methylation caller for
630 Bisulfite-Seq applications. *Bioinformatics*. 2011 Jun 1;27(11):1571-2. doi:
631 10.1093/bioinformatics/btr167. PubMed PMID: 21493656; PubMed Central PMCID:
632 PMC3102221.
- 633 26. Akalin A, Kormaksson M, Li S, et al. methylKit: a comprehensive R package for the
634 analysis of genome-wide DNA methylation profiles. *Genome biology*. 2012 Oct
635 3;13(10):R87. doi: 10.1186/gb-2012-13-10-r87. PubMed PMID: 23034086; PubMed Central
636 PMCID: PMC3491415.
- 637 27. Cavalcante RG, Sartor MA. annotatr: genomic regions in context. *Bioinformatics*.
638 2017 Aug 1;33(15):2381-2383. doi: 10.1093/bioinformatics/btx183. PubMed PMID:
639 28369316; PubMed Central PMCID: PMC5860117.

- 640 28. Kent WJ, Sugnet CW, Furey TS, et al. The human genome browser at UCSC. *Genome*
641 *research*. 2002 Jun;12(6):996-1006. doi: 10.1101/gr.229102. PubMed PMID: 12045153;
642 PubMed Central PMCID: PMC186604.
- 643 29. Sandoval J, Heyn H, Moran S, et al. Validation of a DNA methylation microarray for
644 450,000 CpG sites in the human genome. *Epigenetics*. 2011 Jun;6(6):692-702. PubMed
645 PMID: 21593595.
- 646 30. Meng Z, Wang D, Liu W, et al. Perinatal exposure to Bisphenol S (BPS) promotes
647 obesity development by interfering with lipid and glucose metabolism in male mouse
648 offspring. *Environmental research*. 2019 Mar 21;173:189-198. doi:
649 10.1016/j.envres.2019.03.038. PubMed PMID: 30921577.
- 650 31. Milic S, Lulic D, Stimac D. Non-alcoholic fatty liver disease and obesity: biochemical,
651 metabolic and clinical presentations. *World journal of gastroenterology*. 2014 Jul
652 28;20(28):9330-7. doi: 10.3748/wjg.v20.i28.9330. PubMed PMID: 25071327; PubMed
653 Central PMCID: PMC4110564.
- 654 32. Cohen JC, Horton JD, Hobbs HH. Human fatty liver disease: old questions and new
655 insights. *Science*. 2011 Jun 24;332(6037):1519-23. doi: 10.1126/science.1204265. PubMed
656 PMID: 21700865; PubMed Central PMCID: PMC3229276.
- 657 33. Ahmed S, Atlas E. Bisphenol S- and bisphenol A-induced adipogenesis of murine
658 preadipocytes occurs through direct peroxisome proliferator-activated receptor gamma
659 activation. *International journal of obesity*. 2016 Oct;40(10):1566-1573. doi:
660 10.1038/ijo.2016.95. PubMed PMID: 27273607.
- 661 34. Helies-Toussaint C, Peyre L, Costanzo C, et al. Is bisphenol S a safe substitute for
662 bisphenol A in terms of metabolic function? An in vitro study. *Toxicology and applied*
663 *pharmacology*. 2014 Oct 15;280(2):224-35. doi: 10.1016/j.taap.2014.07.025. PubMed PMID:
664 25111128.

- 665 35. Peyre L, Rouimi P, de Sousa G, et al. Comparative study of bisphenol A and its
666 analogue bisphenol S on human hepatic cells: a focus on their potential involvement in
667 nonalcoholic fatty liver disease. *Food and chemical toxicology : an international journal*
668 published for the British Industrial Biological Research Association. 2014 Aug;70:9-18. doi:
669 10.1016/j.fct.2014.04.011. PubMed PMID: 24793377.
- 670 36. Zhao C, Tang Z, Yan J, et al. Bisphenol S exposure modulate macrophage phenotype
671 as defined by cytokines profiling, global metabolomics and lipidomics analysis. *The Science*
672 *of the total environment*. 2017 Aug 15;592:357-365. doi: 10.1016/j.scitotenv.2017.03.035.
673 PubMed PMID: 28319722.
- 674 37. Pu Y, Gingrich JD, Steibel JP, et al. Sex-Specific Modulation of Fetal Adipogenesis
675 by Gestational Bisphenol A and Bisphenol S Exposure. *Endocrinology*. 2017 Nov
676 1;158(11):3844-3858. doi: 10.1210/en.2017-00615. PubMed PMID: 28938450; PubMed
677 Central PMCID: PMC5695840.
- 678 38. Zhang Z, Lin L, Gai Y, et al. Subchronic bisphenol S exposure affects liver function in
679 mice involving oxidative damage. *Regulatory toxicology and pharmacology : RTP*. 2018
680 Feb;92:138-144. doi: 10.1016/j.yrtph.2017.11.018. PubMed PMID: 29199064.
- 681 39. Meng Z, Wang D, Yan S, et al. Effects of perinatal exposure to BPA and its
682 alternatives (BPS, BPF and BPAF) on hepatic lipid and glucose homeostasis in female mice
683 adolescent offspring. *Chemosphere*. 2018 Aug 17;212:297-306. doi:
684 10.1016/j.chemosphere.2018.08.076. PubMed PMID: 30145421.
- 685 40. Karrer C, Roiss T, von Goetz N, et al. Physiologically Based Pharmacokinetic (PBPK)
686 Modeling of the Bisphenols BPA, BPS, BPF, and BPAF with New Experimental Metabolic
687 Parameters: Comparing the Pharmacokinetic Behavior of BPA with Its Substitutes.
688 *Environmental health perspectives*. 2018 Jul;126(7):077002. doi: 10.1289/EHP2739. PubMed
689 PMID: 29995627; PubMed Central PMCID: PMC6108829.

- 690 41. Song Y, Xie P, Cai Z. Metabolism of bisphenol S in mice after oral administration.
691 Rapid communications in mass spectrometry : RCM. 2017 Dec 26. doi: 10.1002/rcm.8051.
692 PubMed PMID: 29280213.
- 693 42. Oh J, Choi JW, Ahn YA, et al. Pharmacokinetics of bisphenol S in humans after single
694 oral administration. Environment international. 2018 Mar;112:127-133. doi:
695 10.1016/j.envint.2017.11.020. PubMed PMID: 29272776.
- 696 43. Kurt Z, Barrere-Cain R, LaGuardia J, et al. Tissue-specific pathways and networks
697 underlying sexual dimorphism in non-alcoholic fatty liver disease. Biology of sex differences.
698 2018 Oct 22;9(1):46. doi: 10.1186/s13293-018-0205-7. PubMed PMID: 30343673; PubMed
699 Central PMCID: PMC6196429.
- 700 44. Zhang J, Zhang Y, Sun T, et al. Dietary obesity-induced Egr-1 in adipocytes facilitates
701 energy storage via suppression of FOXC2. Scientific reports. 2013;3:1476. doi:
702 10.1038/srep01476. PubMed PMID: 23502673; PubMed Central PMCID: PMC3600596.
- 703 45. Gokey NG, Lopez-Anido C, Gillian-Daniel AL, et al. Early growth response 1 (Egr1)
704 regulates cholesterol biosynthetic gene expression. The Journal of biological chemistry. 2011
705 Aug 26;286(34):29501-10. doi: 10.1074/jbc.M111.263509. PubMed PMID: 21712389;
706 PubMed Central PMCID: PMC3190990.
- 707 46. Magee N, Zhang Y. Role of early growth response 1 in liver metabolism and liver
708 cancer. Hepatoma research. 2017;3:268-277. doi: 10.20517/2394-5079.2017.36. PubMed
709 PMID: 29607419; PubMed Central PMCID: PMC5877465.
- 710 47. Zhang Y, He J, Zhao J, et al. Effect of ApoA4 on SERPINA3 mediated by nuclear
711 receptors NR4A1 and NR1D1 in hepatocytes. Biochemical and biophysical research
712 communications. 2017 May 27;487(2):327-332. doi: 10.1016/j.bbrc.2017.04.058. PubMed
713 PMID: 28412351; PubMed Central PMCID: PMC5956904.

714 48. Wang PW, Hung YC, Wu TH, et al. Proteome-based identification of apolipoprotein
715 A-IV as an early diagnostic biomarker in liver fibrosis. *Oncotarget*. 2017 Oct 24;8(51):88951-
716 88964. doi: 10.18632/oncotarget.21627. PubMed PMID: 29179490; PubMed Central PMCID:
717 PMC5687660.

718 49. Damiri B, Holle E, Yu X, et al. Lentiviral-mediated RNAi knockdown yields a novel
719 mouse model for studying Cyp2b function. *Toxicological sciences : an official journal of the*
720 *Society of Toxicology*. 2012 Feb;125(2):368-81. doi: 10.1093/toxsci/kfr309. PubMed PMID:
721 22083726; PubMed Central PMCID: PMC3262856.

722 50. Desai M, Jellyman JK, Ross MG. Epigenomics, gestational programming and risk of
723 metabolic syndrome. *International journal of obesity*. 2015 Apr;39(4):633-41. doi:
724 10.1038/ijo.2015.13. PubMed PMID: 25640766.

725 51. Kochmanski J, Marchlewicz EH, Savidge M, et al. Longitudinal effects of
726 developmental bisphenol A and variable diet exposures on epigenetic drift in mice.
727 *Reproductive toxicology*. 2017 Mar;68:154-163. doi: 10.1016/j.reprotox.2016.07.021.
728 PubMed PMID: 27496716; PubMed Central PMCID: PMC5290281.

729 52. Carone BR, Fauquier L, Habib N, et al. Paternally induced transgenerational
730 environmental reprogramming of metabolic gene expression in mammals. *Cell*. 2010 Dec
731 23;143(7):1084-96. doi: 10.1016/j.cell.2010.12.008. PubMed PMID: 21183072; PubMed
732 Central PMCID: PMC3039484.

733 53. Michaud EJ, van Vugt MJ, Bultman SJ, et al. Differential expression of a new
734 dominant agouti allele (Aiapy) is correlated with methylation state and is influenced by
735 parental lineage. *Genes & development*. 1994 Jun 15;8(12):1463-72. PubMed PMID:
736 7926745.

737 54. Cheung HH, Davis AJ, Lee TL, et al. Methylation of an intronic region regulates miR-
738 199a in testicular tumor malignancy. *Oncogene*. 2011 Aug 4;30(31):3404-15. doi:
739 10.1038/onc.2011.60. PubMed PMID: 21383689; PubMed Central PMCID: PMC3117973.

740 55. Zhang G, Pradhan S. Mammalian epigenetic mechanisms. *IUBMB life*. 2014
741 Apr;66(4):240-56. doi: 10.1002/iub.1264. PubMed PMID: 24706538.

742 56. Guil S, Esteller M. DNA methylomes, histone codes and miRNAs: tying it all
743 together. *The international journal of biochemistry & cell biology*. 2009 Jan;41(1):87-95. doi:
744 10.1016/j.biocel.2008.09.005. PubMed PMID: 18834952.

745 57. Yang X, Han H, De Carvalho DD, et al. Gene body methylation can alter gene
746 expression and is a therapeutic target in cancer. *Cancer cell*. 2014 Oct 13;26(4):577-90. doi:
747 10.1016/j.ccr.2014.07.028. PubMed PMID: 25263941; PubMed Central PMCID:
748 PMC4224113.

749 58. Molina-Molina JM, Amaya E, Grimaldi M, et al. In vitro study on the agonistic and
750 antagonistic activities of bisphenol-S and other bisphenol-A congeners and derivatives via
751 nuclear receptors. *Toxicology and applied pharmacology*. 2013 Oct 1;272(1):127-36. doi:
752 10.1016/j.taap.2013.05.015. PubMed PMID: 23714657.

753 59. Roelofs MJ, van den Berg M, Bovee TF, et al. Structural bisphenol analogues
754 differentially target steroidogenesis in murine MA-10 Leydig cells as well as the
755 glucocorticoid receptor. *Toxicology*. 2015 Mar 2;329:10-20. doi: 10.1016/j.tox.2015.01.003.
756 PubMed PMID: 25576683.

757 60. Eladak S, Grisin T, Moison D, et al. A new chapter in the bisphenol A story: bisphenol
758 S and bisphenol F are not safe alternatives to this compound. *Fertility and sterility*. 2015
759 Jan;103(1):11-21. doi: 10.1016/j.fertnstert.2014.11.005. PubMed PMID: 25475787.

760 61. Breher-Esch S, Sahini N, Trincone A, et al. Genomics of lipid-laden human
761 hepatocyte cultures enables drug target screening for the treatment of non-alcoholic fatty liver

762 disease. BMC medical genomics. 2018 Dec 14;11(1):111. doi: 10.1186/s12920-018-0438-7.
763 PubMed PMID: 30547786; PubMed Central PMCID: PMC6295111.

764 62. Li J, Liu G, Zhang F, et al. Role of glycoprotein 78 and cidec in hepatic steatosis.
765 Molecular medicine reports. 2017 Aug;16(2):1871-1877. doi: 10.3892/mmr.2017.6834.
766 PubMed PMID: 28656280; PubMed Central PMCID: PMC5561988.

767 63. Chen A, Chen X, Cheng S, et al. FTO promotes SREBP1c maturation and enhances
768 CIDEC transcription during lipid accumulation in HepG2 cells. Biochimica et biophysica acta
769 Molecular and cell biology of lipids. 2018 May;1863(5):538-548. doi:
770 10.1016/j.bbalip.2018.02.003. PubMed PMID: 29486327.

771

Graphical Abstract

